Excitonic absorption in CdTe-based piezoelectric quantum wells

R. André, J. Cibert, and Le Si Dang
Laboratoire de Spectrométrie Physique, Université Joseph Fourier, Grenoble 1, Boîte Postale 87, F-38 402 Saint Martin d'Hères Cedex, France
(Received 10 January 1995; revised manuscript received 11 July 1995)

We have investigated excitonic effects in piezoelectric quantum wells by using a two-parameter variational approach. One parameter is used to describe the spatial extension of the exciton, and the other one to characterize its anisotropy. It is shown that in wide piezoelectric quantum wells, all excitonic effects are controlled by the quantum-confined Stark effect, which tends to localize electrons and holes on opposite interfaces of the quantum well. Hence, in contrast to the case of square quantum wells, excitons in wide piezoelectric quantum wells have an enhanced two-dimensional character, with a binding energy inversely proportional to the well width. We have also calculated exciton absorption using one or two variational parameters, or simply electron-hole overlap integrals. It is found that only the two-parameter variational approach can provide a good quantitative agreement with exciton absorption data we have measured in CdTe square quantum wells and piezoelectric quantum wells.

I. INTRODUCTION

Excitonic effects are certainly among the most studied topics of low-dimensional semiconductor physics. The behavior of excitons as a function of quantum-well (QW) widths L_z is fairly well understood. In the limit of infinite L_z, the exciton is three dimensional (3D) and characterized by an isotropic envelope wave function. As L_z decreases, confinement effects become more important, enhancing the 2D character of the exciton and, consequently, its anisotropy aspect. The simplest way to describe excitonic properties in QW's is to use a variational approach. Very good insights into the exciton problem have thus been obtained with the trial function $\exp(-r/\lambda)$ for the $1s$ exciton envelope function. λ is a variational parameter describing the spatial extension of the exciton, and r is the relative electron-hole separation, given by $r=(x^2+y^2)^{1/2}$ for a 2D situation (infinite barrier and vanishing L_z), or $r=(x^2+y^2+z^2)^{1/2}$ for a 3D situation (infinite L_z), where x, y, and z are the relative electron-hole coordinates, z being the coordinate along the growth axis.[1] However, in realistic QW's the situation is neither 2D nor 3D, and another expression of r is better adapted, i.e., $r=(x^2+y^2+\alpha z^2)^{1/2}$.[2,3] α is a second variational parameter which is a measure of the dimensionality of the exciton, taking values between the two limits $\alpha=0$ for the 2D case and $\alpha=1$ for the 3D case. Note that such a two-parameter variational approach has been used also to describe excitonic anisotropy in double-QW structures.[4,5]

In this paper we present a study of excitonic effects in piezoelectric QW's. It is only recently that the piezoelectric effect in strained semiconductor heterostructures has been theoretically investigated,[6] and firmly established by optical measurements.[7–10] Built-in fields as high as 10^5 V/cm can be easily introduced inside strained heterostructures grown along a polar axis such as (111) or (112). Thus excitonic absorptions are more sensitive to an applied electric field or to photocreated carriers, which makes this type of structure very attractive to device applications.[11] Piezoelectric QW's are also interesting for physical studies. For example, for a given value of the built-in field, increasing the width of a piezoelectric QW results in a progressive separation of electrons and holes, i.e., a continuous tuning from a type-I configuration (with a strong overlap of the electron and hole wave functions) to a type-II one, for which the electron-hole overlap decreases without significant change in the shape of the one-electron and the one-hole wave functions. We have calculated excitonic effects in piezoelectric QW's. The two-parameter variational approach described above has been adopted because we need accurate exciton wave functions for absorption calculations. In contrast to the case of nonpiezoelectric type-I QW's, it is found that the dimensionality parameter α goes to zero for increasing L_z. This enhanced 2D character of excitons in wider piezoelectric QW's is a result of the quantum-confined Stark effect, which strongly localizes electrons and holes on opposite QW interfaces.[12] For this reason, the binding energy of excitons will vary as $1/L_z$ in the regime of strong quantum-confined Stark effect, causing an increase of the spatial extension parameter λ roughly as $L_z/2$.

We have also compared our calculations to excitonic absorption measured in (111)- and (112)-oriented CdTe-based piezoelectric QW's, as well as in (100)- oriented CdTe based QW's. A good quantitative agreement is obtained without any fitting parameters, which supports our choice of the two-parameter variational approach. The rest of the paper is organized as follows. In Sec. II we present the variational approach used to calculate the properties of excitons in piezoelectric QW's. In Sec. III we discuss results from model calculations, with emphasis on the well-width dependence of excitonic effects. In Sec. IV we compare our calculations to excitonic absorption data on CdTe-based piezoelectric QW's and nonpiezoelectric QW's. We also discuss results from calculations using either one variational parameter or simple

electron-hole overlap integrals. Finally we present our conclusions in Sec. V.

II. THEORY

We will consider the case of a single piezoelectric QW embedded in strain-free barriers. We assume that potentials are proportional to Fz in the QW and flat in the barriers, F being piezoelectric field and z the coordinate along the growth axis (see Fig. 1). Within the effective-mass approximation the Hamiltonian of an exciton can be expressed as

$$H_{\rm exc}=H_e+H_h+H_{eh} , \tag{1}$$

where

$$H_e=-\frac{\hbar^2}{2m_e}\frac{\partial^2}{\partial z_e^2}+V_e(z_e)+eF(z_e) ,$$

$$H_h=-\frac{\hbar^2}{2m_h}\frac{\partial^2}{\partial z_h^2}+V_h(z_h)-eF(z_h) ,$$

$$H_{eh}=-\frac{e^2}{4\pi\varepsilon_0\varepsilon\sqrt{z^2+\rho^2}}-\frac{\hbar^2}{2\mu}\left[\frac{1}{\rho}\frac{\partial}{\partial\rho}\left[\rho\frac{\partial}{\partial\rho}\right]+\frac{1}{\rho^2}\frac{\partial^2}{\partial\theta^2}\right] .$$

Here e is the magnitude of the electron charge; ε is the static dielectric constant; $z_e(z_h)$ is the z coordinate of the electron (hole); (z,ρ,θ) are cylindrical coordinates describing the relative motion of electron and hole with $\rho^2=x^2+y^2$; $m_e(m_h)$ is the effective mass of the electron (hole) in the z direction, μ is the reduced exciton effective mass in the plane of the layers (see discussion in Sec. IV), i.e., $1/\mu=1/m_{e\parallel}+1/m_{h\parallel}$ where $m_{e\parallel}$ ($m_{h\parallel}$) is the in-plane effective mass of the electron (hole); and $V_e(z_e)[V_h(z_h)]$ is the rectangular well potential for the electron (hole). $F(z_{e,h})$ is a function defined by $f(z_{e,h})=Fz_{e,h}$ for $z_{e,h}$ in the QW and $F(z_{e,h})=0$ for $z_{e,h}$ in the barriers. The effective masses and the dielectric constants are assumed to be the same in the barriers and in the well. As usual the center-of-mass kinetic energy in the plane has been omitted in (1).

The exciton Hamiltonian (1) is solved variationally by using the following trial wave function:

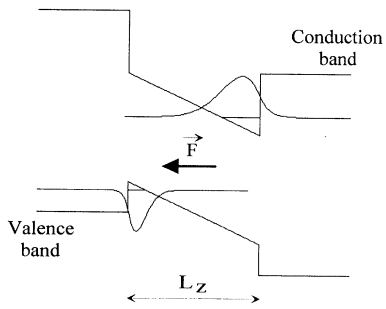

FIG. 1. Schematic diagram of the ground-state energy levels and envelope functions of electrons and holes in a piezoelectric quantum well. F is the built-in field, and L_z is the well width. It is assumed that potentials outside the quantum well are flat on the scale of L_z.

$$\phi_{\rm exc}(z_e,z_h,\mathbf{r})=\frac{1}{\sqrt{N}}\Psi_e(z_e)\Psi_h(z_h)g(\mathbf{r}) . \tag{2}$$

N is the normalization factor. The function $\Psi_e(z_e)$ $[\Psi_h(z_h)]$ is the ground state solution of H_e $[H_h]$, formed by linear combinations of Airy functions in the well and decreasing exponentials in the barriers.[13] The trial function g is a 1s-like hydrogenic function with two variational parameters α and λ:[2,3]

$$g(\mathbf{r})=\exp(-\sqrt{r^2+\alpha z^2}/\lambda) . \tag{3}$$

The parameter α is a measure of the exciton dimensionality: $\alpha=0$ for the 2D case and $\alpha=1$ for the 3D case. The parameter λ is a measure of the exciton spatial extension. Its value should be the 3D Bohr radius for infinite well width in the absence of electric field. Recently excitonic effects in piezoelectric QW's have been calculated by a variational approach using either a purely 2D ($\alpha=0$) or 3D ($\alpha=1$) trial function g.[14] It will be shown below that α takes intermediate values and only goes to zero for infinitely large L_z.

The ground-state solution of (1) is obtained by minimizing energies with respect to α and λ. The multidimensional integrals required for the energy calculations have been evaluated numerically. Thus one obtains the binding energy of the exciton as well as parameters describing its wave function, which will be useful for absorption calculations. Let $E_{\rm exc}$ be the exciton energy. The probability of excitonic absorption of an incident photon, whose energy is E, is given by[15]

$$W(E)=\frac{\pi\hbar a E_p e^2}{3\varepsilon_0 cnm_0 E}\frac{|\langle\psi_e|\psi_h\rangle|^2}{N}\delta(E_{\rm exc}-E) , \tag{4}$$

where n is the refractive index, c is the velocity of light, m_0 is the free-electron mass, a is a constant equal to 1 for the heavy-hole exciton and $\frac{1}{3}$ for the light-hole exciton, and E_p is the Kane matrix element. In practice excitonic transitions are broadened, so that we characterize the experimental absorption by the following quantity:

$$A=\int\frac{I_0(E)-I_t(E)}{I_0(E)}dE . \tag{5}$$

Here $I_0(E)$ and $I_t(E)$ are the intensities of the incident and transmitted photon of energy E, respectively. In Eq. (5), we do not take into account excitonic effects on the reflectance of the sample, since their contributions to the integrated absorption are found to be negligibly small (see Sec. IV and Fig. 7 below). The quantity A, expressed in units of energy, is the relevant physical parameter to be compared directly to the calculated integrated absorption probability $\int W(E)dE$.

III. EXCITONS IN PIEZOELECTRIC QW'S

In this section we discuss excitonic effects in piezoelectric QW's from model calculations. We use parameter values typical for (111)-oriented $CdTe/Cd_{0.8}Mn_{0.2}Te$ QW's: $m_e=0.096$, $m_h=1$, $\mu=0.08$, $V_e=185$ meV, and $V_h=92$ meV. All energies and lengths have been normal-

ized to the CdTe 3D exciton Rydberg $R_y^* = 11$ meV and Bohr radius $a_b = 63$ Å, respectively. Figures 2–5 show the evolution of parameters α and λ, binding energies, and absorptions as a function of the well width L_z. Calculations have been made for several values of the piezoelectric field F, including $F = 0$ which corresponds to the case of square QW's.

First let us discuss the case of square QW's ($F = 0$) to check for consistency with well-known results. In our model calculations, confinement effects are maximum for $L_z \approx 0.5a_b - 1a_b$: the dimensionality parameter α is minimum and close to 0.4 (Fig. 2); the spatial extension parameter λ is slightly smaller than a_b (Fig. 3); the binding energy is maximum and equal to about $2R_y^*$ (Fig. 4). This shows that the exciton is fairly anisotropic, in an intermediate regime between ideal 2D and 3D. For large L_z, all physical parameters of the model converge to the anticipated 3D values: α approaches 1, which means that the exciton becomes more isotropic; λ is now equal to one Bohr radius; the binding energy decreases to $1R_y^*$; and absorption is increasing linearly with L_z (Fig. 5). Concerning absorption, the minimum observed in Fig. 5 is similar to that calculated by Andreani, d'Andrea, and del Sole for excitons in CuCl thin films.[16] These authors pointed out that the well-width dependence of the oscillator strength per unit area, f, should have a minimum. The reason is that f varies continuously between two limits corresponding to small L_z and large L_z. For small L_z, f increases with confinement effects. For large L_z (in the 3D regime), f increases linearly with L_z because the oscillator strength per unit volume is constant.

In piezoelectric QW's, the exciton picture is completely different and it is instructive to begin with the dimensionality parameter α. As shown in Fig. 2, the well-width dependence of α first follows that of square QW's before separating from it to go down to zero for larger L_z. This complex variation is well explained by the competition between confinement effects and quantum-confined Stark effect. For sufficiently small L_z ($\leq a_b$), confinement effects are dominant so the exciton is not much altered by the

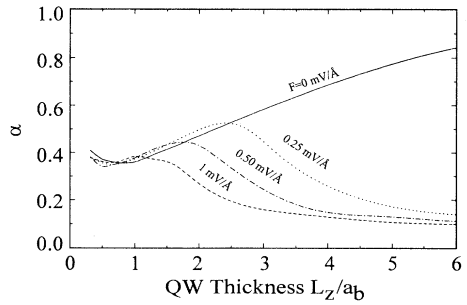

FIG. 2. Variation of the dimensionality parameter α as a function of the well width, for different values of the piezoelectric field $F = 0$, 0.25, 0.5, and 1 mV/Å. The well width is expressed in units of the 3D Bohr radius a_b. Note that for square quantum wells ($F = 0$) the parameter α increases towards 1 with increasing well width. For piezoelectric quantum wells ($F \neq 0$), α goes the opposite way, showing an increased anisotropic character of the excitons.

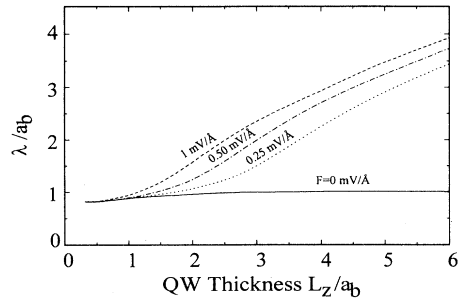

FIG. 3. Variation of the spatial extension parameter λ as a function of the well width, for different values of the piezoelectric field $F = 0$, 0.25, 0.5, and 1 mV/Å. The well width and the parameter λ are expressed in units of the 3D Bohr radius a_b. For square quantum wells ($F = 0$), the parameter λ is close to a_b and does not vary much with increasing well width, whereas it continuously increases for piezoelectric quantum wells ($F \neq 0$).

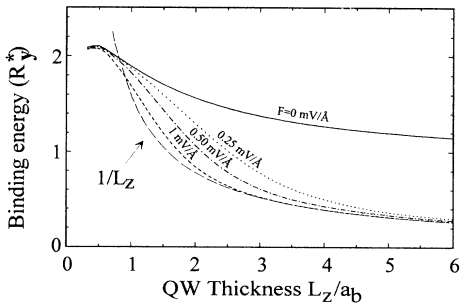

FIG. 4. Variation of the ground-state exciton binding energy as a function of the well width, for different values of the piezoelectric field $F = 0$, 0.25, 0.5, and 1 mV/Å. The well width is expressed in units of the 3D Bohr radius a_b, and the binding energy in units of the 3D Rydberg R_y^*. A variation of the binding energy as $1/L_z$ is also shown for comparison.

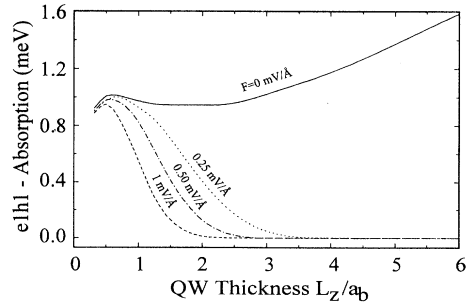

FIG. 5. Variation of the integrated absorption of the ground-state exciton as a function of the well width, for different values of the piezoelectric field $F = 0$, 0.25, 0.5, and 1 mV/Å. The well width is expressed in units of the 3D Bohr radius a_b.

electric field: α varies as in square QW's, independently of the piezoelectric field F values. However, the quantum-confined Stark effect is more effective with increasing L_z, since electrons and holes can be pushed towards opposite QW interfaces.[12,17] Consequently, Coulomb correlations of electron-hole pairs will be reduced along the electric field (or z) direction, and the parameter α will decrease. As expected transitions to this regime of strong quantum-confined Stark effect occur at smaller L_z for piezoelectric QW's with larger built-in fields, typically when the electron-hole overlap is reduced by about a factor of 3.

The above qualitative description of excitons in piezoelectric QW's also allows one to understand the variation of other physical parameters. In the regime of strong quantum-confined Stark effect, electrons and holes are mostly localized in the triangular part of the QW, as shown schematically in Fig. 1. Then, if we neglect for a while the extension of the wave functions along z and the Coulomb correlation along this same direction, excitons can be viewed as being formed from two planes of opposite charges separated by about the well width L_z. As a result, an increase of L_z will reduce the Coulomb interaction between electrons and holes, causing an increase of the spatial extension of the exciton. This dependence is indeed reproduced by the calculations, as shown in Fig. 3: more precisely it is found that the parameter λ varies as $L_z/2$ in our model calculations. Now, how should the binding energy of the exciton vary in the regime of strong quantum-confined Stark effect? One can note that the binding energy results from a balance between the kinetic energy and the Coulomb energy, which vary as $1/\lambda^2$ and $1/\lambda$, respectively. In fact, for a 3D exciton, the kinetic energy can be written as $R_y^*(a_b/\lambda)^2$ and the Coulomb energy as $-2R_y^*(a_b/\lambda)$. Then if λ is very large, as is the case for large fields and wide piezoelectric QW's, the binding energy of the exciton will be dominated by the Coulomb contribution. Indeed, the $1/L_z$ dependence observed for the binding energy in Fig. 4 confirms that it corresponds mainly to the Coulomb interaction between electrons and holes separated by an average distance L_z.

The absorption of the $e1h1$ exciton will decrease with increasing well width also, but with a rate much faster than for the binding energy. To illustrate this point we show in Fig. 6 a log-log plot of absorption versus binding energy, using data from Figs. 3 and 4. Binding energies have been normalized to the 3D R_y^* and absorptions to that of a square QW of 100 Å. It can be seen that, depending on the piezoelectric field, absorption decreases three or four orders of magnitude faster than binding energy. This feature, previously reported in Ref. 14, can be explained as follows. Absorption, as described by Eq. (4), involves not only the electron-hole overlap, but also the normalization factor N which increases with λ. In fact, N is proportional to λ^2 in a purely 2D exciton model ($\alpha=0$). Then the variation of absorption can be approximated by [overlap/λ^2], which presents a much stronger well-width dependence than the variation ($1/\lambda$) for the binding energy.

Finally we would like to comment on the use of a two-parameter variational approach. It is interesting to note that α in Fig. 2 decreases down to about 0.1, i.e., very close to the value zero of the ideal 2D case. This means that excitonic effects under strong quantum-confined Stark effect or wide piezoelectric QW's are better described with a 2D exciton envelope wave function than with a 3D one. However, in the range of situations we have explored, α remains finite. As Coulomb correlations along the z direction vary as $\sqrt{\alpha}/\lambda$, this means that the electron-hole overlap along this direction is enhanced by Coulomb interaction, even in wide piezoelectric QW's. Setting $\alpha=0$ suppresses this enhancement effect: this will not change the calculated binding energy much, but will underestimate the calculated absorption since this latter is more sensitive to the accuracy of the wave functions. We will go back to this point in the next section.

IV. EXCITONIC ABSORPTION IN CdTe PIEZOELECTRIC QW'S

In this section we compare our calculations to absorption data measured on samples listed in Table I. These samples are $CdTe/Cd_{1-x}Zn_x$ Te or $CdTe/Cd_{1-x}Mn_xTe$ single QW's or multiple QW's grown along a (100), (111), or (112) axis by molecular-beam epitaxy. For details of the growth conditions, see Ref. 18. Values of physical parameters used in the calculations are given in Table II. Valence-band offsets have been taken to be zero for CdTe/ZnTe (Ref. 19) and equal to 30% of the total band-gap difference for CdTe/MnTe.[20] The Luttinger Hamiltonian and the Bir and Pikus Hamiltonian have been used to describe the valence-band dispersion in QW's. For the samples in Table I, the QWs are under biaxial compression, which is imposed by the strain-free barriers. This compression produces typical valence-band splittings of 30 meV or larger, with the heavy-hole band as the ground state. In-plane dispersions of valence sub-

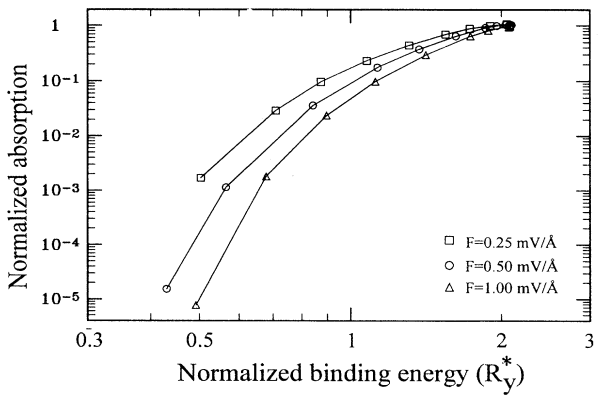

FIG. 6. Log-log plot of the integrated absorption of the ground-state exciton (same data as in Fig. 5) versus its binding energy (same data as in Fig. 4), for different values of the piezoelectric field $F=0.25$, 0.5, and 1 mV/Å. Absorption is normalized to that of a 100 Å square quantum well, and the binding energy is expressed in units of the 3D Rydberg. Note the strong variation of the exciton absorption as compared to its binding energy.

TABLE I. Experimental and calculated absorptions for a series of CdTe-based QW's. These QW's are under biaxial strains and exhibit piezoelectric fields when the growth direction is different from (100). Error bars on calculated absorption values result from ±5% on QW widths and on the piezoelectric fields. Error bars are on experimental values come from the choice of the baseline for the determination of the integrated absorption (see dashed line on Fig. 7).

Sample	QW number	Growth axis	QW width (Å)	Piezoelectric field (mV/Å)	Barrier material	Absorption[a] (meV) (experiment)	Absorption[a] (meV) (calculation)	α	λ (Å)
$S1$	40	(111)	115	0.82	$Cd_{0.83}Mn_{0.17}Te$	0.045±0.005	0.05±0.01	0.38	97
$S2$	40	(211)	90	1.56	$Cd_{0.60}Mn_{0.40}Te$	0.07±0.02	0.07±0.02	0.33	89
$S3$	40	(111)	101	0.94	$Cd_{0.82}Mn_{0.18}Te$	0.10±0.01	0.07±0.02	0.39	90
$S4$	40	(111)	92	0.97	$Cd_{0.82}Mn_{0.18}Te$	0.17±0.01	0.12±0.02	0.42	84
$S5$	5	(100)	141	0	ZnTe	0.51±0.02	0.56±0.01	0.52	78
$S6$	1	(100)	100	0	$Cd_{0.88}Zn_{0.12}Te$	0.73±0.14	0.57±0.01	0.56	78
$S7$	10	(100)	47	0	$Cd_{0.83}Mn_{0.17}Te$	0.78±0.13	0.75±0.01	0.36	62

[a]For one QW.

bands have been calculated for various directions of the wave vector,[21] using the axial approximation. This approximation, derived by Lipari and Altarelli[22] for bulk materials, allows one to average out warping effects of in-plane dispersions in strained QW's.[23] As expected, band mixing effects are small for the ground-state heavy-hole subband, so that its dispersion can be reasonably fitted by a parabola to deduce an in-plane effective mass $m_{h\|}$.

Figure 7 shows the reflectivity and transmission spectra of sample $S3$ at 1.8 K. This sample contains 4 (111)-oriented $CdTe/Cd_{0.82}Mn_{0.18}Te$ QW's. The widths of QW's and barriers are 100 and 1000 Å, respectively, and the piezoelectric field is $F=0.94$ mV/Å. Excitonic effects are not well pronounced in the reflectivity spectrum, in contrast to the transmission spectrum for which two strong absorption peaks can be clearly observed. They have been assigned to transitions between the ground electron subband $e1$ and the heavy-hole subbands $h1$ and $h2$. Note that both transitions are of comparable intensity as a result of the strong quantum-confined Stark effect. Dotted lines in the figure represent baselines we have used to estimate the $e1h1$ integrated absorption. It can be seen that the reflectivity contribution can be neglected here: first, excitonic effects on the reflectance of the sample are about 5% of excitonic effects on the transmittance at the absorption peak (in Fig. 7, the average reflectance is about 25%); second, the reflectance has a derivativelike shape which results in a small integrated signal. Therefore only the transmission spectrum has been used to calculate the experimental integrated absorption A given by Eq. (5).

Results of calculations are given in Table I. In order to have a direct comparison we have plotted calculated absorptions versus measurements in Fig. 8. The diagonal solid line represents a perfect fit. The results of the present calculation are represented by points with error bars, which mainly come from uncertainties on the values of the piezoelectric field and the well width (±5%), and from the choice of the base line $I_0(E)$. We have used the Kane matrix element $E_p=20$ eV in Eq. (5),[24] and the static dielectric constant $\varepsilon=10$.[25] The agreement is very good, especially as there are no fitted parameters in Eq. (4).

TABLE II. Parameters used for absorption calculations. $\delta E_{VB}/\delta E_g$ is the ratio between the valence-band discontinuity, at the $CdTe/Cd_{1-x}Zn_xTe$ or $CdTe/Cd_{1-x}Mn_xTe$ interface, and the total band-gap difference. The band-gap differences are calculated using $E_G(Cd_{1-x}Zn_xTe)=1606+525x+260x^2$ (meV) (Ref. 27) and $E_g(Cd_{1-x}Mn_xTe)=1606+1592x$ (meV) (Ref. 28). Lattice parameters for $Cd_{1-x}Zn_xTe$ or $Cd_{1-x}Mn_xTe$ alloys are assumed to follow Vegard's law.

Luttinger parameters[a,b]	Deformation potentials[b] (eV)	Lattice parameter (Å)	Elastic stiffness[c,b] (GPa)	$\delta E_{VB}/\delta E_g$
$\gamma_1=4.8\pm0.4$	$a=3.3$[d]	$a_{CdTe}=6.481$[e]	$C_{11}=56.6$	$CdTe/Cd_{1-x}Zn_xTe$: 0%[f]
$\gamma_2=1.5\pm0.3$	$b=1.1$[g]	$a_{ZnTe}=6.104$[h]	$C_{12}=39.6$	$CdTe/Cd_{x-1}Mn_xTe$: 30%[i]
$\gamma_3=1.9\pm0.2$	$d=3.2$[j]	$a_{MnTe}=6.334$[k]	$c_{44}=20.7$	

[a]Reference 29.
[b]Parameters for CdTe.
[c]Reference 31.
[d]Reference 30.
[e]Reference 34.
[f]Reference 19.
[g]Reference 32.
[h]Reference 34.
[i]Reference 20.
[j]Reference 33.
[k]Reference 28.

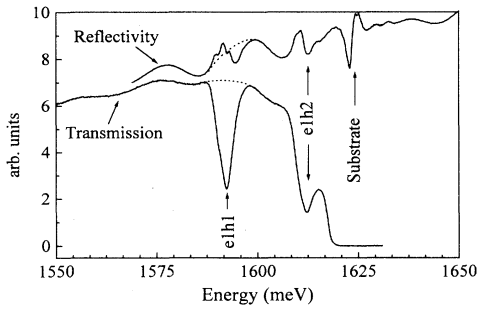

FIG. 7. Transmission and reflectivity spectra at $T=1.8$ K of sample $S3$ which contains 40 (111)-oriented $CdTe/Cd_{0.82}Mn_{0.18}Te$ QW's. The widths of QW's and barriers are 100 and 1000 Å, respectively, and the piezoelectric field is $F=0.94$ mV/Å. $e1h1$ and $e1h2$ lines correspond to excitonic transitions between the ground electron subband $e1$ and the heavy-hole subbands $h1$ and $h2$. The dotted lines represent the baselines used to estimate excitonic effects related to $e1h1$ (see text).

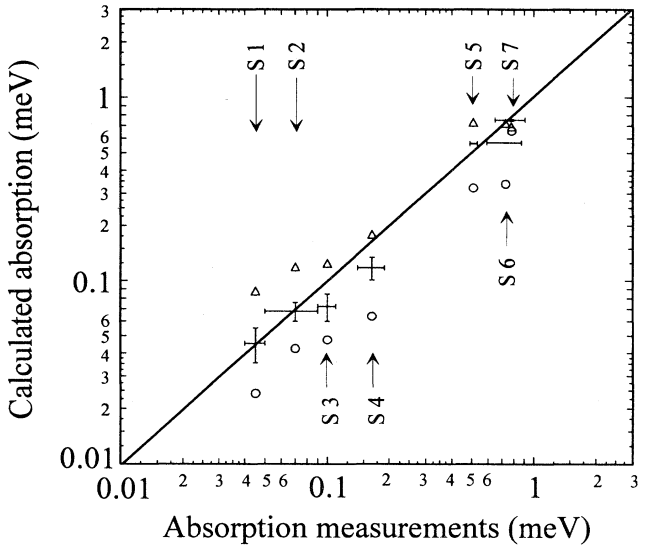

FIG. 8. Comparison of exciton absorption data in CdTe square quantum wells [grown along (100)] and CdTe piezoelectric quantum wells [grown along (111) and (112)] to three different model calculations. Points with error bars correspond to calculations using two variation parameters (α and λ), circles to calculations using one variational parameter (λ) with $\alpha=0$, and triangles to calculations using electron-hole overlap integrals. A perfect fit in this plot is represented by the solid line. Absorption is always underestimated by the 2D variational model ($\alpha=0$) and overestimated by the overlap model.

For illustrative purpose we show also in Fig. 8 absorptions calculated either variationally with a 2D exciton model (parameter $\alpha=0$) or with a simple model based on electron-hole overlap.[26] In the latter case the normalization factor N in Eq. (4) is set constant and equal to the square of the 3D Bohr radius. Both calculations give the right qualitative evolution of absorption but not absolute values. As discussed in sec. IV, the actual variation of the absorption is steeper than that of the overlap integrals because the exciton extension in the QW plane depends strongly on the well width (through the normalization factor N). On the other hand, the 2D model systematically underestimates the absorption because it does not take into account the electron-hole correlation along the z axis.

V. CONCLUSIONS

In this paper we have investigated excitonic effects in piezoelectric QW's by using a two-parameter variational approach. We have shown that the 2D character of excitons is strongly enhanced with increasing well width. This behavior, completely opposite to that of excitons in square QW's, is due to the quantum-confined Stark effect which spatially separates the electron-hole pair in piezoelectric QW's. In the regime of strong quantum-confined Stark effect, electrons and holes are mostly localized at opposite QW interfaces: excitons can then be viewed as formed by two planes of opposite charges separated by the well width L_z. Increasing L_z decreases the binding energy and increases the spatial extension of the exciton. As a result, the absorption of the $e1h1$ exciton decreases at a much faster rate than the binding energy, faster than the simple overlap of the uncorrelated electron-hole pair envelope functions. Finally, our calculations have been compared to absorption data in (100)-, (111)-, and (112)-oriented CdTe QW's. While the absorption is systematically underestimated in a purely 2D exciton model, it is found that a quantitative agreement is obtained without any fitted parameter with the two-parameter variational model.

ACKNOWLEDGMENTS

This work has been completed within the CEA-CNRS joint group "Microstructures de Semiconducteurs II-VI." We would like to thank G. Fishman for the calculations of valence-band dispersions and numerous illuminating discussions.

[1]G. Bastard, E. E. Mendez, L. L. Chang, and L. Esaki, Phys. Rev. B **26**, 1974 (1982).
[2]Y. Shinozuka and M. Matsuura, Phys. Rev. B **28**, 4878 (1983).
[3]M. Grundmann and D. Bimberg, Phys. Rev. B **38**, 13 486 (1988).
[4]T. Kamizato and M. Matsuura, Phys. Rev. B **40**, 8378 (1989).
[5]Y. Takahashi, Y. Kato, S. S. Kano, S. Fukatsu, Y. Shiraki, and R. Ito, J. Appl. Phys. **76**, 2299 (1994).
[6]D. L. Smith and C. Mailhiot, Rev. Mod. Phys. **62**, 173 (1990).
[7]B. K. Laurich, K. Elcess, C. G. Fonstad, J. G. Beery, C. Mailhiot, and D. L. Smith, Phys. Rev. Lett. **62**, 649 (1989).
[8]X. Chen, P. J. Parbrook, C. Trager-Cowan, B. Henderson, K. P. O'Donnell, M. P. Halsall, J. J. Davies, J. E. Nicholls, P. J. Wright, and B. Cockayne, Semicond. Sci. Technol. **5**, 997

(1990).
[9]R. André, C. Deshayes, J. Cibert, Le Si Dang, S. Tatarenko, and K. Saminadayar, Phys. Rev. B **42**, 11 392 (1990).
[10]T. S Moise, L. J. Guido, R. C. Barker, J. O. White, and A. R. Kost, Appl. Phys. Lett. **60**, 2637 (1992).
[11]K. W. Goossen, E. A. Caridi, T. Y. Chang, J. B. Stark, D. A. B. Miller, and R. A. Morgan, Appl. Phys. Lett **56**, 715 (1990).
[12]D. A. B. Miller, D. S. Chemla, T. C. Damen, A. C. Gossard, W. Wiegmann, T. H. Wood, and C. A. Burrus, Phys. Rev. Lett. **53**, 2173 (1984).
[13]J. Cibert, R. André, C. Bodin, Le Si Dang, G. Feuillet, and P. H. Jouneau, Phys. Scr. **T49**, 487 (1993).
[14]P. Boring, K. J. Moore, P. Bigenwald, B. Gil, and K. Woodbridge, J. Phys. (France) IV **3**, C5-249 (1993).
[15]R. J. Elliott, in *Theory of Excitons,* edited by C. G. Kuper and G. D. Whitfield (Academic, New York, 1963); R. J. Elliott, Phys. Rev. **108**, 1384 (1957).
[16]L. C. Andreani, A. d'Andrea, and R. del Sole, Phys. Lett. A **168**, 451 (1992).
[17]J. A. Brum and G. Bastard, Phys. Rev. B **31**, 3893 (1985).
[18]J. Cibert, R. André, C. Deshayes, Le Si Dang, H. Okumura, S. Tatarenko, G. Feuillet, P. H. Jouneau, R. Mallard, and K. Saminadayar, J. Cryst. Growth **117**, 424 (1992).
[19]H. Mariette, F Dal'bo, N. Magnea, G. Lentz, and H. Tuffigo, Phys. Rev. B **38**, 12 443 (1988).
[20]A. Wasiela, P. Peyla, Y. Merle d'Aubigné, J. E. Nicholls, D. E. Ashenford, and B. Lunn, Semicond. Sci. Technol. **7**, 571 (1992).
[21]G. Fishman (unpublished).
[22]N. O. Lipari and M. Altarelli, Phys. Rev. B **15**, 4883 (1977).
[23]D. A. Broido and L. J. Sham, Phys. Rev. B **31**, 888 (1985); M. Altarelli, U. Ekenberg, and A. Fasolino, *ibid.* **32**, 5138 (1985).
[24]C. Hermann and C. Weisbuch, in *Optical Orientation,* edited by F. Meier and B. P. Zakharchenya (Elsevier, Amsterdam, 1984).
[25]B. Segall and T. F. Marple, in *Physics and Chemistry of II-VI Compounds,* edited by M. Aven and J. S. Prener (North-Holland, Amsterdam, 1967).
[26]L. Vina, E. E. Mendez, W. I. Wang, L. L. Chang, and L. Esaki, J. Phys. C **20**, 2803 (1987).
[27]V. A. Tyagai, O. V. Snitko, V. N. Bondarenko, N. I. Vitrikhovskii, V. B. Popov, and A. N. Krasiko, Fiz. Tverd. Tela (Leningrad) **16**, 1373 (1974) [Sov. Phys. Solid State **16**, 885 (1974)].
[28]J. K. Furdyna, J. Appl. Phys. **64**, R29 (1988).
[29]Le Si Dang (unpublished).
[30]H. Mathieu, J. Allegre, A. Chatt, P. Lefebvre, and J. P. Faurie, Phys. Rev. B **38**, 7740 (1988).
[31]R. D. Greenough and S. B. Palmer, J. Phys. D **6**, 587 (1973).
[32]Y. Merle d'Aubigné, H. Mariette, N. Magnéa, H. Tuffigo, R. T. Cox, G. Lentz, Le Si Dang, J. L. Pautrat, and A. Wasiela, J. Cryst. Growth **101**, 650 (1990).
[33]B. Gil and D. J. Dunstan, Semicond. Sci. Technol. **6**, 428 (1991).
[34]*Semiconductors,* edited by O. Madelung and M. Schulz, Landolt-Börnstein, New Series, Group III, Vol. 22, Pt. a (Springer-Verlag, Berlin, 1987).